Informaticae Abstracta. ISSN: 3061-8533
Año 2026, Vol. 4, No. 1, pp. 83-98
JUL | DIC 2025
doi: https://doi.org/10.36677/ia.v4n1.28940

Evaluation of the different time-travel approaches used in geotechnical seismic testing

Contreras-Ferreyra, D. U.*; Pastor-Gómez, N.; Chávez-Negrete, C.; Martínez-Rojas, A.

Información del Artículo

Recibido: 1 de febrero, 2026
Aceptado: 5 de mayo, 2026

Palabras clave: seismic testing, signal processing, Fourier transform, Hilbert transform, instrumentation

Resumen

Soil stiffness can be evaluated using various techniques, among which seismic geophysical tests stand out for their simplicity and applicability. Their fundamental principle is to determine the travel times of seismic waves between points within the soil mass using transducers. In this research, a laboratory seismic protocol was used to analyze three classic approaches to defining travel times: start-to-start, maximum peak-to-peak, and minimum peak-to-peak. The test was conducted on a well-graded gravel specimen using low-cost accelerometers and impact-generated compression waves. Thirty seismic determinations were obtained and processed by applying a low-pass filter derived from the frequency spectrum via the Fourier transform. Additionally, the envelope of the seismic signals obtained via the Hilbert transform was examined, and two alternative approaches based on this technique were proposed. The results show that the start-to-start method offers the best statistical consistency, whereas the maximum peak-to-peak approach is the least reliable, even generating negative travel times. Although the approaches derived from the Hilbert transform did not yield consistent results, their potential applicability in scenarios involving different transducers or types of seismic waves is proposed. Overall, the study contributes to the discussion of selecting interpretation criteria for laboratory seismic protocols.

Introduction and background

Seismic testing is one of the most widely used techniques in geotechnical engineering for estimating the mechanical behavior of a material under low strain [1, 2, 3]. Essentially, by measuring the propagation velocity of artificial seismic waves, mechanical behavior parameters such as the modulus of elasticity, shear modulus, and Poisson's ratio can be determined [4].

These methodologies range from field tests, such as downhole or crosshole tests, to laboratory tests, such as the Bender Elements test [5]. In all cases, a seismic wave is generated at a point in the soil mass, either by an impact or by a small displacement caused by a transducer. The moment this wave is produced is recorded over time by a sensor (obtaining a signal known as the input or transmitter signal). Similarly, a receiver sensor is placed at another location in the soil being analyzed. The purpose of this receiver sensor is to record the time it takes for the seismic wave to travel from its point of origin to the location of the receiver sensor (output or receiver signal). The time difference recorded between the two sensors, along with their distance, yields the wave velocity [6, 7].

In theory, defining this differential arrival time for the sensor would seem straightforward. However, certain phenomena associated with the signals from these sensors, such as noise, frequency, and the type of filtering, among others, can affect the clear detection of this time. Therefore, different approaches have been proposed to define these seismic wave arrival times in the sensor signals. Some of the most common are the “start-to-start,” “maximum peak-to-peak,” and “minimum peak-to-peak” approaches [8, 9]. Graphically, these approaches are shown in Figure 1. As can be seen, these approaches are based on identifying characteristic points in the signal from both the sensor where the seismic excitation originates and the receiving sensor. These points represent the start of the excitation, as well as the first maximum and minimum peaks of both signals. While in synthetic signals, such as the one shown in Figure 1, the time differentials for any approach are very similar, in real tests, notable differences between these times can be observed.

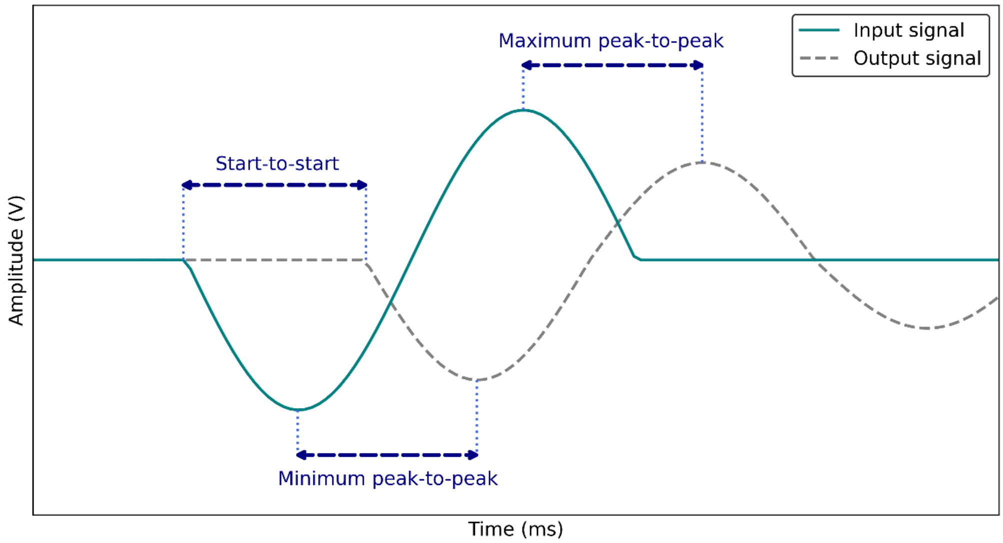

Figura 1: Determination of seismic wave arrival times (based on Fernández-Lavín et al. [8]).

In this work, a statistical analysis was performed on the results obtained using three different classic methodologies for determining seismic wave travel time. A laboratory specimen was prepared from granular material, with two accelerometers embedded to detect seismic vibrations. To generate the waves, the specimen was impacted on its surface, similar to field tests. This generated a compressional wave (P-wave) that traveled throughout the specimen. Subsequently, the signals were filtered using a Fourier filter to improve their geometry, and the arrival times were then determined. Furthermore, the Hilbert transform was applied to the filtered signals to propose two additional approaches to determining travel times.

Seismic protocol configuration

Test specimen

To obtain the seismic signals, a specimen was prepared as shown schematically in Figure 2. As shown in the figure, two sensors were embedded in a compacted soil specimen within a rigid, cylindrical mold, 34 cm high and 15 cm in diameter. The sensors are 22 cm apart. Their operation and interface are explained in the following section.

The soil of the specimen consisted of well-graded, non-plastic crushed gravel, classified as GW under the Unified Soil Classification System (USCS). It was compacted in several layers, approaching its maximum dry density (2.17 g/cm^3). Once compaction finished, a circular steel plate, 15 cm in diameter and 1.25 cm thick, was placed on top of the specimen. To generate seismic waves, this plate was struck vertically with a 16 oz. rubber mallet. This simulated a downhole test [9] on a laboratory specimen, with the seismic wave first being detected by the upper transducer (Sensor A) and then, after a certain time interval (Δt), by the lower transducer (Sensor B). It should be noted that, because the impact generated vertical stress within the soil mass, the resulting wave was a P-wave (compressional wave).

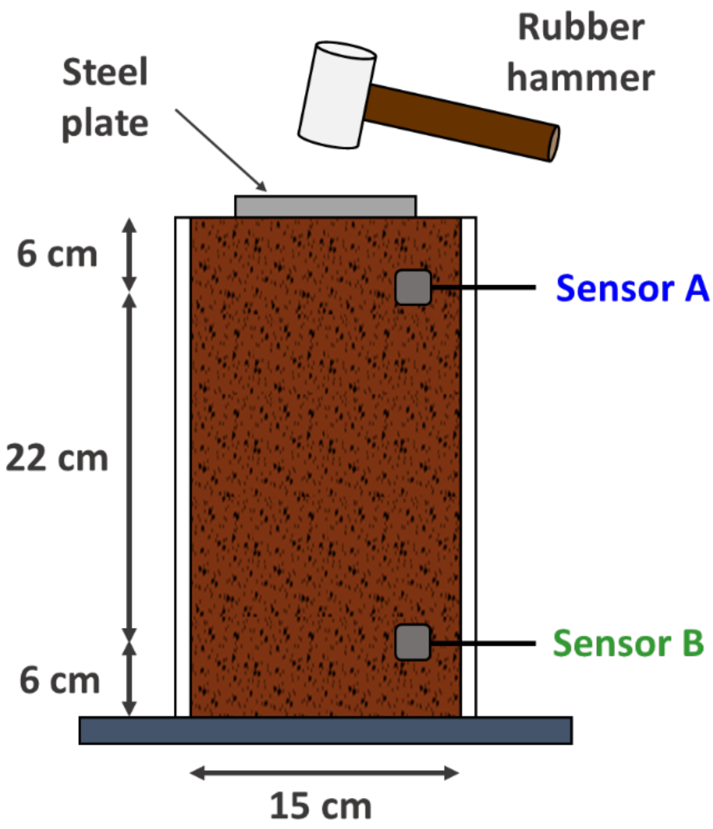

Figura 2: Schematic representation of the test specimen and the seismic protocol developed.

Seismic transducers

Typically, seismic wave detection uses transducers whose primary purpose is to capture small-scale vibrations or displacements. The most used transducers include geophones, accelerometers, and piezoelectric sensors. In this research, the ADXL335 accelerometer was used. This small sensor (2.1 cm in length and 1.5 cm in height) has been used in various applications that require detecting vibrations or impacts. According to the manufacturer, this sensor is an analog device with three channels for measuring acceleration in the three orthogonal directions, with a measurement range of ± 3 times the acceleration due to gravity. This sensor requires an external power supply in the range of 3.3 to 5V, and since it emits an analog signal, it can be connected to virtually any conventional data acquisition board. However, in seismic tests, whether in the field or in the laboratory, a high sampling rate is usually used due to the high frequency of the generated seismic waves.

In the implemented seismic protocol, a National Instruments NI-USB-6009 data acquisition card was used. This device, which connects to a computer via USB, can detect both digital and analog signals and has a 12-bit resolution. For analog signals, such as those emitted by the accelerometer, a single-ended connection was implemented, allowing the card to operate within a voltage range of ± 10 volts. Therefore, no signal conditioner was required between the accelerometer and the card. Furthermore, since the proposed protocol uses a pair of accelerometers, a sampling rate of 24,000 samples per second was defined, pushing the card to its maximum capacity, as it allows a sampling rate of 48,000 samples per second distributed across its input channels. Likewise, a sampling interval of 2 seconds was set, which is sufficient time to activate the sensors, generate seismic excitation, and detect the resulting signal.

An important point to highlight is that because the sensors were embedded in the soil mass as it was compacted, it was necessary to protect them from damage during compaction. Thus, each sensor was enclosed within a cylindrical steel capsule with an internal diameter of 2.5 cm. These capsules had a base (where the sensor was placed) and a top part that served as a lid for the base, with the two parts threaded together. Once the sensor was encapsulated, it did not suffer any damage during the soil compaction, nor did it affect such process. Figure 3 shows the sensor housed inside the capsule.

Figura 3: ADXL335 accelerometers housed inside the steel capsule.

Seismic signals

Figure 4a shows an example of the typical signals captured by both sensors during a seismic test, considering the previously set duration of 2 seconds. To observe in more detail the moment the seismic wave reaches the sensors, Figure 4b shows a close-up of that region of the signals. Furthermore, once the signal is recorded, it is common practice to remove the extremes, focusing primarily on the aforementioned region, since this is the area of interest, thereby maximizing the computational resources used to process these signals.

As illustrated in Figure 4b, seismic waves are fleeting, lasting less than 150 milliseconds before fading. Analyzing the signals, a slightly higher initial amplitude is observed in the signal from Sensor A (blue line). This is consistent with the specimen's configuration, since this sensor is closer to the seismic wave's origin and is expected to record the wave with greater intensity. Conversely, once the seismic wave reaches Sensor B, it has already dissipated somewhat as it travels through the soil mass, resulting in a slightly lower signal amplitude there. Furthermore, both signals tend to follow the same oscillatory motion until the seismic wave finally dissipates completely.

Another point to mention is that for geotechnical seismic tests, where the primary goal is to detect travel time, the signal units can be expressed in voltage without needing to convert them to displacements, velocities, or acceleration. This is because the main objective is to determine the time difference between the arrival times of seismic waves at the sensors, and from this value, obtain the seismic wave velocity. Therefore, such conversion is unnecessary, and this approach is adopted in the present research.

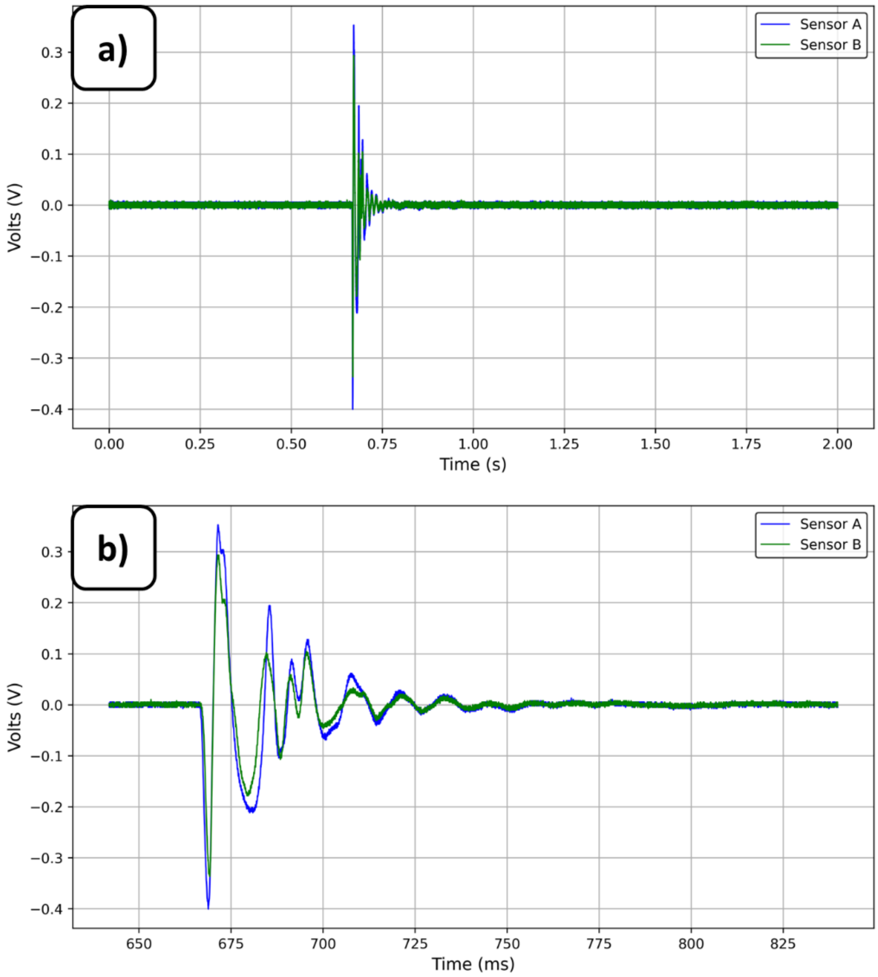

Figura 4: Example of signals from a typical seismic test. a) Original signal acquired; b) Cropping of the extremes of both signals.

Signal processing and time differentials

Fourier transform

Although signals like those shown in Figure 4 are considered to have relatively well-defined geometry, seismic wave signal analysis typically employs some processing or filtering techniques to improve signal quality by eliminating noise and achieving greater definition of the signal geometry [10]. In this research, it was observed that removing noise (high-frequency, low-amplitude oscillations) was particularly important for obtaining more accurate and precise seismic wave arrival times.

For this purpose, one of the most widely used techniques in digital signal processing was employed: the Fourier transform. This technique is based on the principle that all signals are sums of different sinusoidal components [11, 12]. Applying this transform, a signal defined in the time domain is expressed in the frequency domain, allowing each frequency and its contribution level to be defined [13]. Once the signal is defined in the frequency domain, a filtering process can be applied, followed by the inverse Fourier transform, so that the signal under analysis is again defined in the time domain [14].

Figure 5 shows the signal from Sensor A, as shown in Figure 4, but now defined in its frequency spectrum, displaying all the signal's components. As can be seen, the highest-contribution frequencies are low. Therefore, if any of these components are eliminated or altered, the geometry of the resulting signal will change considerably from the original. Thus, a low-pass filter was implemented at this point, which attenuates frequencies above a certain threshold, leaving only the low frequencies [15]. Furthermore, since the objective of implementing the Fourier transform was to eliminate noise, which corresponds to high-frequency components, this type of filtering is appropriate for the seismic wave signals observed in this research. As seen in the example in Figure 5, frequencies above 1000 hertz were nullified, which is the most commonly used filtering value for both the signals from Sensor A and Sensor B.

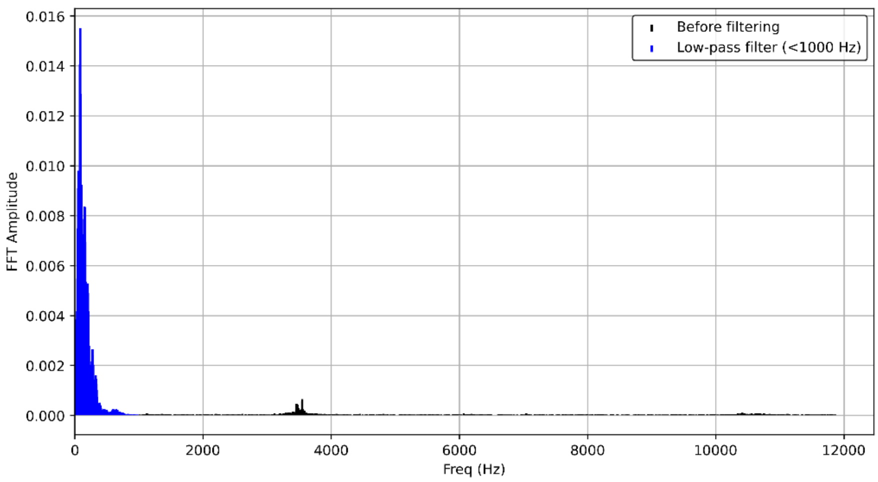

Figura 5: Frequency spectrum of the signal captured by sensor A.

Figure 6 shows the result of the process of removing high frequencies and the subsequent application of the inverse Fourier transform to the signal from Sensor A. As can be seen, the noise shown throughout the signal was noticeably eliminated.

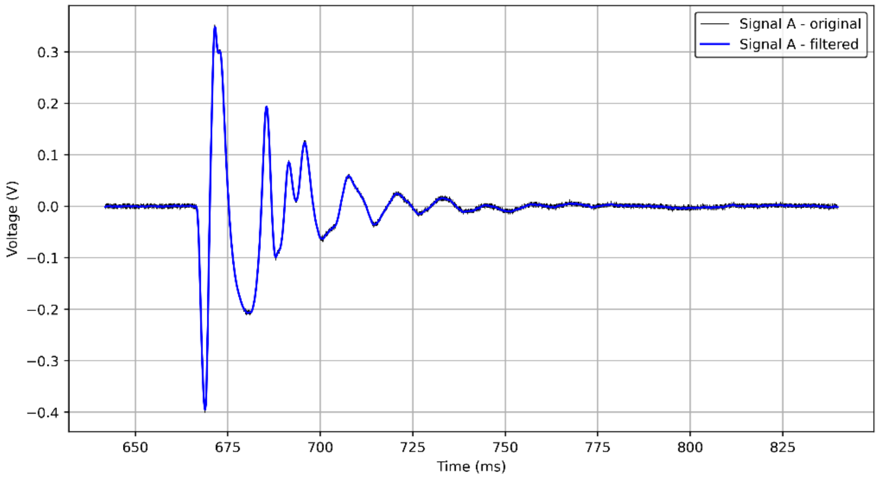

Figura 6: Application of the low-pass filter to signal A.

Finally, Figure 7 shows the filtered signals from both sensors, providing a closer look at the area where the seismic excitation was detected. As shown in this figure, the geometry of both signals improved significantly without drastically altering the signal pattern. This allows for a clearer understanding of the seismic excitation and a better definition of the geometry of the first drop and both negative and positive first peaks, which are essential for this research.

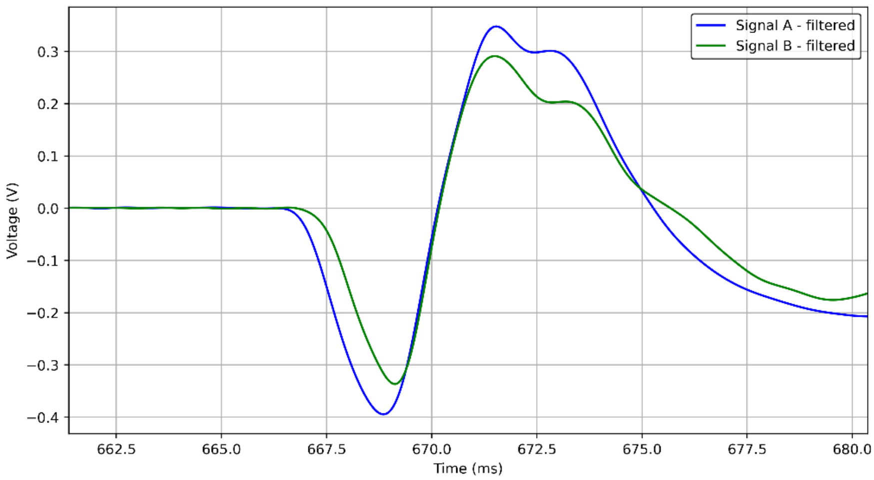

Figura 7: Filtered signals from both sensors.

Hilbert transform

While the signals obtained from the Fourier transform-based filtering process are considered clean and have a defined geometry, other approaches could be explored to analyze these seismic signals from a different perspective, providing an alternative for defining the time differential required to calculate the seismic wave velocity. Even standardized procedures, such as the Bender element test defined in ASTM D8295 [16], allow other techniques to be used.

Based on this argument, the Hilbert transform was used on seismic signals in this work. This technique has been implemented in other areas, such as radiocommunications engineering, and is also applicable to vibration signals [17]. When the Hilbert transform is applied to a signal, the result is an identical-geometry signal with a 90° phase shift relative to the original; that is, an orthogonal signal. This resulting signal, known as the "analytical signal," is complex, as it contains both real and imaginary components. If the magnitude of this signal (absolute value) is obtained, the result is an envelope of the original signal [17, 18, 19].

Figure 8 shows an example of the application of the Hilbert transform and its envelope. As shown in the figure, where the original signal has a sinusoidal amplitude-modulated geometry, the Hilbert transform generates a phase shift in the signal. Subsequently, by evaluating the magnitude of the analyzed signal, an envelope of the signal is obtained. It should be noted that this envelope only corresponds to the positive portion of the signal, since it was obtained from the absolute value of the analytical signal. However, if the signal is symmetric with respect to the horizontal axis, the lower (negative) envelope can be obtained from the negative value of this envelope. It is also important to point out that if the analyzed signal is in the time domain (as is the case with signals obtained by seismic sensors), the Hilbert transform does not produce a change of domain, and therefore does not affect the spectral components of the signal [18].

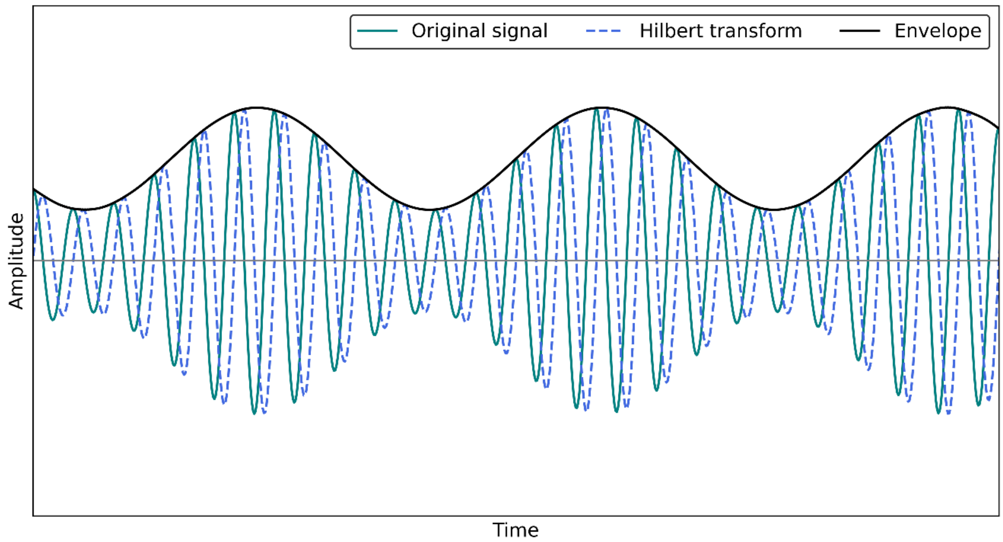

Figura 8: Example of the Hilbert transform in an amplitude-modulated signal and its positive envelope.

For the seismic signals obtained, since they are also symmetric with respect to the time axis, it is sufficient to plot the envelope; therefore, only the positive envelope was considered. Figure 9 shows the implementation of the signal envelope based on the Hilbert transform for the signals obtained after the Fourier filtering process. As shown, the obtained signals exhibit a horizontal separation from each other similar to that observed in the original signals. Furthermore, the maximum peaks are clearly distinguishable in the generated envelopes, which closely coincide with the horizontal midpoint between the minimum and maximum peaks of each signal. Additionally, the amplitude peaks observed in the original signals follow the same previously defined trend, where the envelope of signal A exhibits a greater amplitude compared to envelope B.

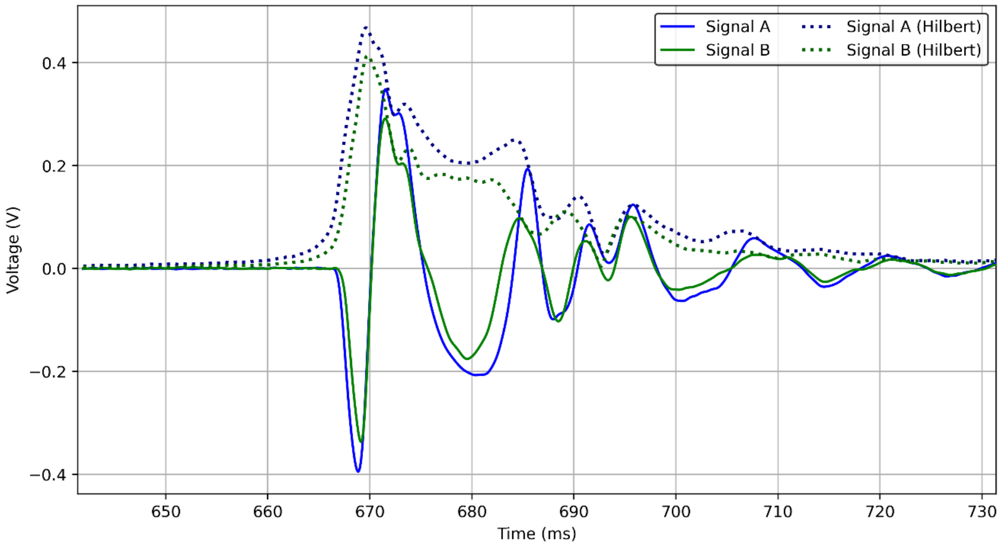

Figura 9: Definition of the envelope through the Hilbert transform for seismic signals.

Time differentials

After applying Fourier filtering and the Hilbert transform to the signals, the seismic wave arrival times were determined for each signal from the two sensors. For this, the traditional approaches to filtering the signals were adopted: "start-to-start," "maximum peak-to-peak," and "minimum peak-to-peak." Likewise, two similar approaches were proposed for the envelopes obtained by the Hilbert transform: "peak-to-peak" and "initial phase-shift." The initial step involves identifying the time at which each signal's envelope reaches its maximum peak. On the other hand, the "initial phase-shift" approach consists of recording the times at which the first slope of each signal begins.

Figure 10 shows the application of the first three classical approaches, while Figure 11 shows the two proposed approaches applied to the resulting envelopes. In all cases, the arrival time at each sensor is recorded in milliseconds, considering that the time differential (Δt) sought in seismic tests corresponds to the difference between the time recorded by sensor B and the time recorded by sensor A.

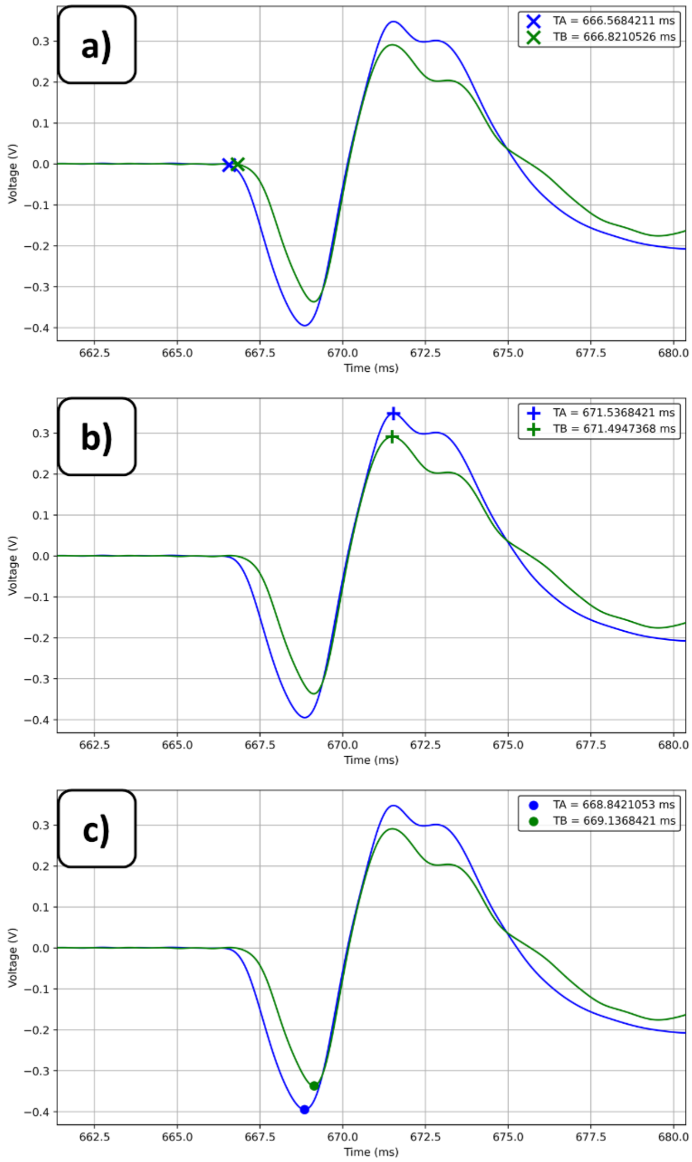

Figura 10: Definition of arrival times by conventional approaches. a) Start-to-start; b) Maximum peak-to-peak; c) Minimum peak-to-peak.

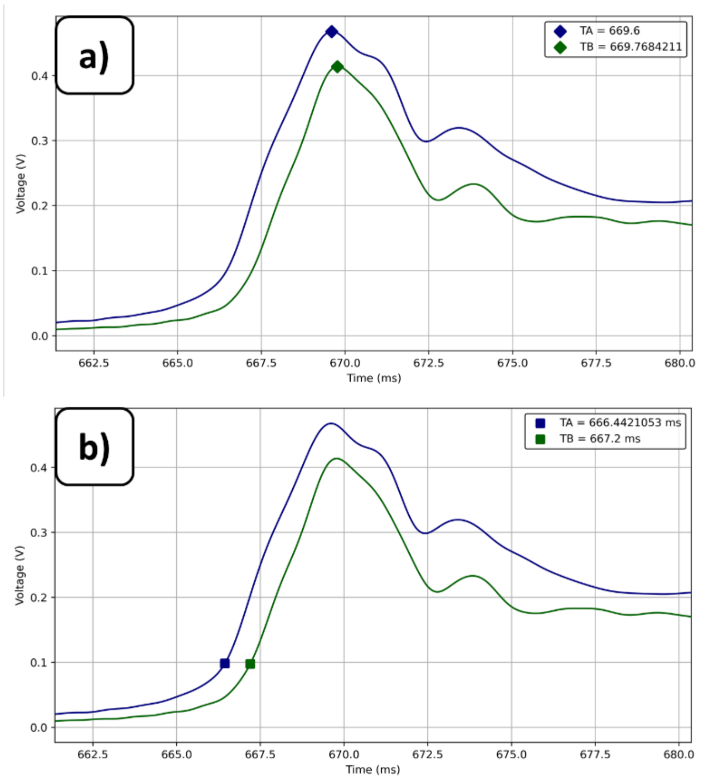

Figura 11: Definition of arrival times using the envelope derived from the Hilbert transform. a) Peak-to-peak; b) Phase-shift.

Analysis of results

A total of 30 seismic determinations were performed, evaluating Δt using the previously mentioned approaches. Table 1 presents the basic descriptive statistics for these data, including measures of central tendency (mean, median, and mode) and common measures of dispersion to assess variability in each data set (range, standard deviation, and coefficient of variation).

Analyzing the measures of central tendency, it is observed that the maximum peak-to-peak approach yields the smallest values for the mean, median, and mode, whereas the maximum peak-to-peak approach using the Hilbert transform yields the highest values, with the other approaches yielding intermediate values. The variation in these values demonstrates that quantifying the time differential is not as trivial as some seismic standards and protocols suggest, and that different techniques can yield different seismic wave velocities for the same material.

However, these measures of central tendency alone do not capture the consistency and variability of each approach; these are quantitatively assessed using measures of dispersion. As shown in Table 1, the approach with the least dispersion, in terms of both standard deviation and coefficient of variation, is “start-to-start,” while “maximum peak-to-peak” has a coefficient of variation of 335.77 %, indicating high variability and dispersion in the data evaluated with this approach. Furthermore, as observed, this approach yielded negative values less than -2 milliseconds. This explains why the lowest values were obtained in the measures of central tendency for this dataset. The practical implication of these negative values is that the seismic wave was apparently first captured by the lower sensor and then by the upper sensor, thus resulting in a negative Δt. This condition is observed in Figure 10b, where the time recorded by sensor B is inferior to that recorded by sensor A. This scenario is far from reality, since sensor B is located farther from the origin of the seismic wave than sensor A; therefore, it is inconsistent to have a negative Δt for this seismic protocol. Due to its high variability, this approach is discarded for further analysis. The other approaches mostly show a moderate coefficient of variation.

Tabla 1: Measures of central tendency and dispersion of the Δt results of the analyzed approaches.

	Start-to-start	Maximum peak-to-peak	Minimum peak-to-peak	Peak-to-peak (Hilbert)	Phase shift (Hilbert)
Mean	0.460012	0.173533	0.389111	0.210381	0.697290
Median	0.484210	0.021053	0.421053	0.210526	0.631579
Mode	0.547368	0.000000	0.421053	0.294737	0.926316
Maximum	0.589474	0.757895	0.631579	0.421053	0.968421
Minimum	0.168421	-2.125590	0.084211	0.000000	0.294737
Range	0.421053	2.883485	0.547368	0.421053	0.673684
Standard deviation	0.099483	0.582683	0.132530	0.113307	0.178037
CV (%)	21.626	335.776	34.060	53.858	25.533

Figure 12 shows the frequency histograms of the time differentials obtained for each approach, illustrating how the data are distributed within each set. It should be noted that the Sturges criterion, which is based on the number of observations, was used to define the intervals for all histograms. In this case, across the 30 seismic measurements, all histograms are divided into 6 intervals.

For the start-to-start approach (Figure 12a), most results are concentrated in the upper end of the range (close to 0.6 ms), while smaller values (0.2–0.3 ms) are less frequent and exhibit a marked left skew. For the minimum peak-to-peak and Hilbert transform peak-to-peak approaches, the time differentials are mainly concentrated in intermediate values, while the extremes are less frequent, although the former has a more pronounced peak toward the arithmetic mean. Finally, the phase-shift approach using the Hilbert transform also exhibits dominant central values, with some occurrences at the upper end, and a wider range of values compared to the other datasets.

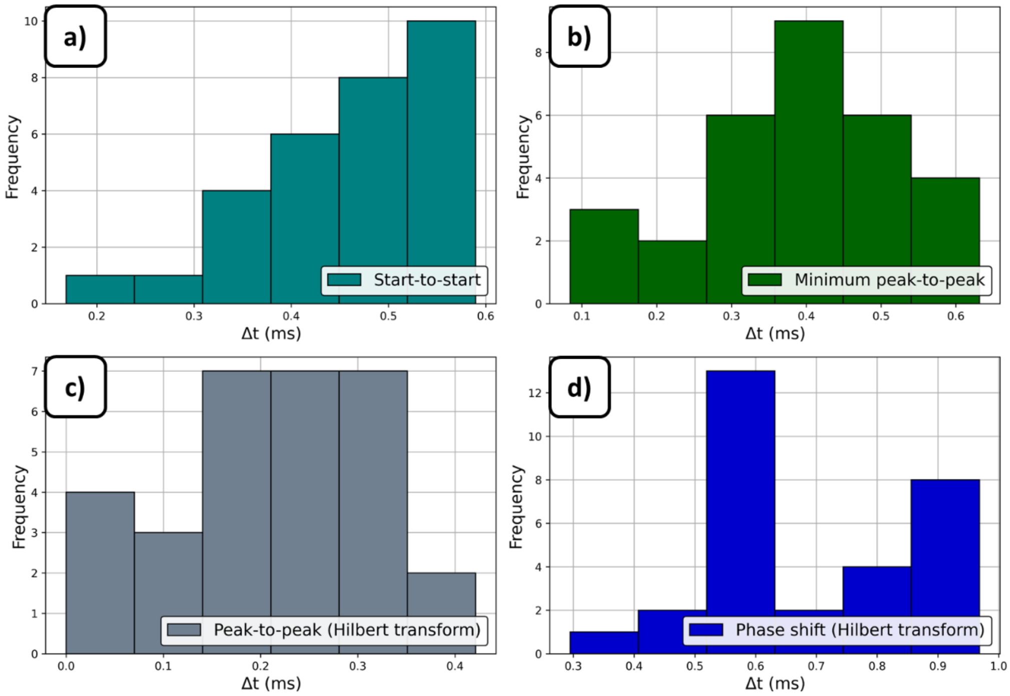

Figura 12: Frequency histograms. a) Start-to-start; b) Minimum peak-to-peak; c) Peak-to-peak (Hilbert transform); d) Phase-shift (Hilbert transform).

Finally, to compare the approaches, Figure 13 shows a box plot. In these plots, the length of the box represents the interquartile range from Q1 to Q3 (or between 25 % and 75 % of the data), while the lines extending from the box (called whiskers) represent the dispersion of the data beyond the quartiles. The center line within the box represents the median of each data set.

This analysis shows that the traditional "Start-to-start" approach yields the most stable and consistent results, exhibiting a low interquartile range and with the mean located roughly in the middle of the box. Furthermore, the whiskers are shorter than those in the other methods. The other classic "minimum peak-to-peak" approach presents a box with a median similar to the "start-to-start" approach, but it shows a larger interquartile range and, while its whiskers are larger, are somewhat symmetrical at both ends. Similarly, the "peak-to-peak Hilbert transform" approach has a low interquartile range (even lower than the "start-to-start" approach), although it can reach very low Δt values, even down to 0, as shown by its range of values in Table 1. Finally, the graph of the phase-shift approach using the Hilbert transform shows the largest box, with a median much higher than the others and a very large range, indicating greater dispersion of results.

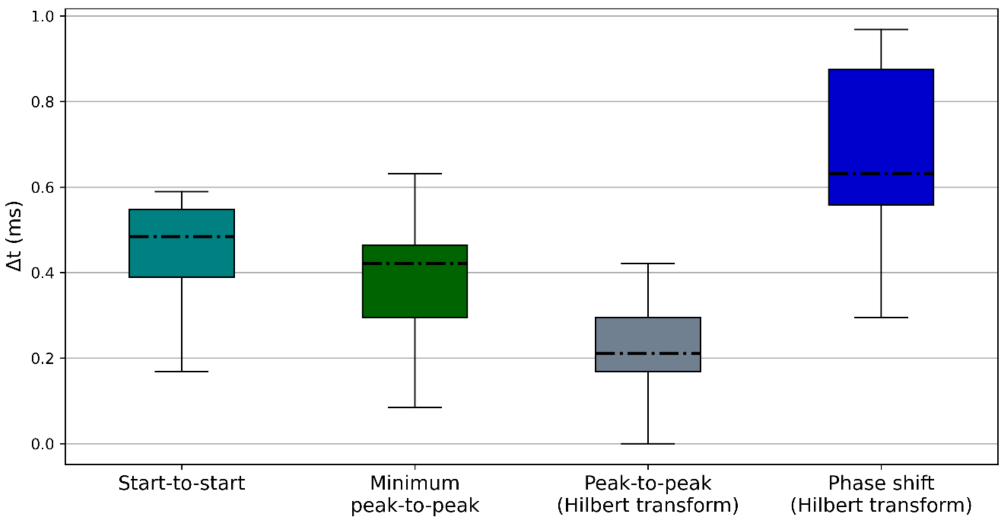

Figura 13: Box plots of the obtained Δt.

Conclusions

The objective of this work was to statistically analyze time-differential results obtained from traditional approaches used in seismic geophysical tests, both in the field and in the laboratory. Additionally, the Hilbert transform was applied to evaluate the sensor-captured signals from a different perspective.

Some of the most relevant conclusions obtained from this work are presented below.

- The ADXL335 sensors are a low-cost and easy-to-implement alternative for seismic wave detection. However, these sensors must be properly encapsulated to prevent damage during soil compaction or from the humid environment in which they are placed. Furthermore, although these sensors were used in this study on a specimen under more controlled conditions, these accelerometers may also have applications in field tests, providing an alternative to other, more expensive transducers.

- Arrival times depend heavily on the shape of the signals. Therefore, factors external to the seismic test, such as the type of seismic wave or the sensor used, can produce waves with slightly varying geometry. Furthermore, these signals sometimes undergo additional mathematical processing, such as computing derivatives or integrals, especially when the sensors measure velocity or acceleration. Consequently, while some approaches did not yield highly accurate results with the proposed seismic protocol, they may be applicable when using other types of transducers.

- A key improvement to the seismic signal geometry was the implementation of the Fourier transform and a subsequent low-pass filter in the frequency domain. This approach significantly reduced signal noise, thereby decreasing the uncertainty in the arrival time estimates. Therefore, this technique is highly recommended for seismic testing.

- Likewise, the Hilbert transform has potential applications in seismic studies. Although the approaches based on this transform were not the most consistent in this research, it is possible that this transform could provide an alternative for signal analysis in other seismic tests where other approaches exhibit significant variations.
- Finally, it is worth noting that the seismic protocol executed using the "start-to-start" approach yields the most reliable results with the least dispersion, making it the recommended approach for this type of test. If complications arise in implementing this approach, the next recommended analysis is the "minimum peak-to-peak" method, and lastly, approaches based on the Hilbert transform.

Direcciones de correo de los autores

CONTRERAS-FERREYRA, D. U.*: Facultad de Ingeniería Civil, Universidad Michoacana de San Nicolás de Hidalgo, Morelia, Michoacán, México
dante.contreras@umich.mx

PASTOR-GÓMEZ, N.: Facultad de Ingeniería Civil, Universidad Michoacana de San Nicolás de Hidalgo, Morelia, Michoacán, México
npastor@umich.mx

CHÁVEZ-NEGRETE, C.: Facultad de Ingeniería Civil, Universidad Michoacana de San Nicolás de Hidalgo, Morelia, Michoacán, México
cachavez@umich.mx

MARTÍNEZ-ROJAS, A.: Facultad de Ingeniería Civil, Universidad Michoacana de San Nicolás de Hidalgo, Morelia, Michoacán, México
alondra.martinez@umich.mx

Referencias

[1] M. Budhu, *Soil Mechanics and Foundations*. Hoboken, NJ: John Wiley & Sons, 2008.

[2] R. E. Hunt, *Geotechnical Investigation Methods: A Field Guide for Geotechnical Engineers*. Boca Raton, FL: CRC Press, 2006.

[3] J. E. Loehr, A. Lutenegger, B. L. Rosenblad y A. Boeckmann, «Geotechnical Site Characterization: Geotechnical Engineering Circular No. 5 (FHWA-NHI-16-072),» National Highway Institute, Federal Highway Administration, Washington, DC, inf. téc., 2016.

[4] C. Vergniault y J. L. Mari, «Shear velocity measurement in boreholes,» en *Well Seismic Surveying and Acoustic Logging*, J. L. Mari, ed., Les Ulis: EDP Sciences, 2018.

[5] A. Sawangsuriya, «Wave propagation methods for determining stiffness of geomaterials,» *Wave Processes in Classical and New Solids*, vol. 44, 2012.

[6] Y. Gao, X. Zheng, H. Wang y W. Luo, «Effect of wave attenuation on shear wave velocity determination using bender element tests,» *Sensors*, vol. 22, n.º 3, pág. 1263, 2022. DOI: 10.3390/s22031263

[7] J. Kumar y N. S. Shinde, «Interpretation of bender elements results by using the sliding Fourier transform method,» *Canadian Geotechnical Journal*, cgj-2018-0733, 2019. DOI: 10.1139/cgj-2018-0733

[8] A. Fernández-Lavín, C. Chamorro-Zurita y E. Ovando-Shelley, «An alternative method to analyze waveforms from bender element tests in soft clays,» *Geotechnical and Geological Engineering*, vol. 42, n.º 1, págs. 43-60, 2024.

[9] ASTM International, «Standard test methods for downhole seismic testing,» ASTM International, West Conshohocken, PA, inf. téc. D7400/D7400M-19, 2019.

[10] V. Joevivek, N. Chandrasekar y R. Jayangondaperumal, «Evaluation of optimal wavelet filters for seismic wave analysis,» *Himalayan Geology*, vol. 37, n.º 2, págs. 176-189, 2016.

[11] A. V. Oppenheim, A. S. Willsky y S. H. Nawab, *Signals & Systems*, 2nd. Upper Saddle River, NJ: Pearson Educación, 1997.

[12] D. Sundararajan, *A Practical Approach to Signals and Systems*. Singapore: John Wiley & Sons, 2009.

[13] R. N. Bracewell, *The Fourier Transform and Its Applications*, 3rd. New York: McGraw-Hill, 2000.

[14] A. Veloni, N. Miridakis y E. Boukouvala, *Digital and Statistical Signal Processing*. Boca Raton, FL: CRC Press, 2018.

[15] L. Tan, *Digital Signal Processing: Fundamentals and Applications*. Burlington, MA: Academic Press, 2007.

[16] ASTM International, «Standard test method for determination of shear wave velocity and initial shear modulus in soil specimens using bender elements,» ASTM International, West Conshohocken, PA, inf. téc. D8295-19, 2019.

[17] H. Luo, X. Fang y B. Ertas, «Hilbert transform and its engineering applications,» *AIAA Journal*, vol. 47, n.º 4, págs. 923-932, 2009.

[18] M. E. Abdulmunem y A. A. Badr, «Hilbert Transform and its Applications: A survey,» *International Journal of Scientific & Engineering Research*, vol. 8, n.º 2, págs. 699-704, 2017.

[19] E. A. Awada, M. H. Alomari y E. Radwan, «Wavelet estimation of THD based on Hilbert transform extraction,» *International Journal of Applied Engineering Research*, vol. 11, n.º 9, págs. 6451-6456, 2016.